

CONSTRAINED COSMOLOGICAL SIMULATIONS OF DARK MATTER HALOS

EMILIO ROMANO-DIAZ^{1,2}, ANDREAS FALTENBACHER³, DANIEL JONES^{2,4}, CLAYTON HELLER⁴,
YEHUDA HOFFMAN¹, AND ISAAC SHLOSMAN²

Submitted to Astrophysical Journal Letters

ABSTRACT

The formation and structure of dark matter (DM) halos is studied by means of constrained realizations of Gaussian fields using N -body simulations. A series of experiments of the formation of a $10^{12}h^{-1}M_{\odot}$ halo is designed to study the dependence of the density profile on its merging history. We confirm that the halo growth consists of violent and quiescent phases, with the density well approximated by the Navarro-Frenk-White (NFW) profile during the latter phases. We find that (1) the NFW scale radius R_s stays constant during the quiescent phase and grows abruptly during the violent one. In contrast, the virial radius grows linearly during the quiescent and abruptly during the violent phases. (2) The central density stays unchanged during the quiescent phase while dropping abruptly during the violent phase. (3) The value of R_s reflects the violent merging history of the halo, and depends on the number of violent events and their fractional magnitudes, independent of the time and order of these events. It does not reflect the formation time of the halo. (4) The fractional change in R_s is a nonlinear function of the fractional absorbed kinetic energy within R_s in a violent event.

Subject headings: cosmology: dark matter — galaxies: evolution — galaxies: formation — galaxies: halos — galaxies: interactions — galaxies: kinematics and dynamics

1. INTRODUCTION

The problem of the formation and structure of dark matter halos constitutes one of the outstanding challenges of modern cosmogony and structure formation models. The problem is easily formulated as what is the outcome of the collapse and virialization of bound perturbations in an otherwise homogenous and isotropic expanding universe. This is further simplified by considering only collisionless non-interacting particles, hereafter referred to as dark matter (DM). The resulting collapsed objects are dubbed here as *halos*. This seemingly simple problem does not easily yield itself to an analytical understanding — the problem addressed here in a series of numerical ‘experiments’.

Analytical and numerical studies of the collapse and virialization of structures in an expanding universe date to the early times of modern cosmogony. The only rigorous and exact analytical solution relevant to the problem is that of a single scale free spherical density perturbation in a Friedmann universe, the so-called secondary infall model (Gunn 1977; Fillmore & Goldreich 1984; Bertschinger 1985) and its application to cosmological models (Hoffman & Shaham 1985, etc.). The shortcoming of the analytical approach prompted the study of the formation of DM halos by means of N -body simulations (White 1976, etc.). The structure of DM halos inferred from a variety of cosmological models and power spectra of the primordial perturbation field was found to be well approximated by a spherically averaged density profile

(Navarro, Frenk & White 1996, 1997, hereafter NFW),

$$\rho(r) = \frac{4\rho_s}{(r/R_s)(1+r/R_s)^2}, \quad (1)$$

where ρ_s is the density at the scale radius R_s . The NFW profile constitutes a universal fit to the structure of DM halos over many orders of magnitudes in mass and at different redshifts. It has been confirmed by numerous N -body simulations, although some modifications have been suggested (most notably Moore et al. 1998). The origin of the NFW profile has been studied in the framework of the secondary infall model (*e.g.*, Nusser & Sheth 1999; Lokas & Hoffman 2000; Nusser 2001; Ascasibar et al. 2004) and the merger scenario (El-Zant 2005). While analytical models necessarily invoke spherical symmetry, simulations emphasize the background asymmetry. This has led us to embark on a series of numerical experiments carefully designed to shed light on the problem.

In this *Letter* we address the role of the merging history in shaping up the density profile. It has been determined that the evolution of DM halos proceeds in two phases, of rapid and slow accretion (Wechsler et al. 2002; Zentner & Bullock 2003; Zhao et al. 2003; Salvador-Solé et al. 2005, and refs. therein). The general understanding that has followed is that an NFW structure is quickly established after the rapid phase and is preserved during the slow accretion. Thus it follows that the emergence and evolution of the NFW profile might depend primarily on the mergers epoch (*e.g.*, El-Zant 2005). This motivates our first study of the formation of DM halos by using constrained simulations. We design a set of numerical experiments in which a given halo of mass $10^{12}h^{-1}M_{\odot}$ (where h is the Hubble’s constant in units of $100 \text{ km s}^{-1}\text{Mpc}^{-1}$) is constrained to follow different merging histories. We then study the different constrained halos and compare the evolution of their density profiles.

¹ Racah Institute of Physics, Hebrew University, Jerusalem 91904, Israel

² Department of Physics & Astronomy, University of Kentucky, Lexington, KY 40506-0055, USA

³ Physics Department, University of California, Santa Cruz, CA 95064, USA

⁴ Department of Physics, Georgia Southern University, Statesboro, GA 30460, USA

The ability to design initial conditions for N -body simulations by constrained realizations of Gaussian fields is the *key* to the ‘experimental’ approach used here. This is done by following the Hoffman & Ribak (1991) algorithm. The design of an experiment starts with the expression of whatever constraints one would like to impose into linear constraints on the primordial perturbation field, which is assumed to be Gaussian within the inflation paradigm. The constrained realization is used to set up the initial conditions by means of the Zel’dovich (1970) approximation. The resulting simulation is referred here as a constrained simulation.

The linear constraints are described in §2, the models are presented in §3 and their analysis in §4. The cosmological implications are discussed in §5.

2. CONSTRAINED SIMULATIONS

We used the updated version of the FTM-4.4 hybrid code (Heller & Shlosman 1994; Heller 1995), with $N \sim 2.1 \times 10^6$. The gravitational forces are computed using the routine `falcoN` (Dehnen 2002), which is about ten times faster than optimally coded Barnes & Hut (1986) tree code. The gravitational softening is $\epsilon = 500$ pc. The addressed issue of the collapse of an individual halo in an expanding Friedmann universe has led us to use vacuum boundary conditions and to perform the simulations with physical coordinates. In these coordinates the cosmological constant, or its generalization as dark energy, should be introduced by an explicit term in the acceleration equation. The FTM code in its present form does not contain a cosmological constant term. This has led us to assume the open CDM (OCDM) model with $\Omega_0 = 0.3$, $h = 0.7$ and $\sigma_8 = 0.9$ (where Ω_0 is the current cosmological matter density parameter and σ_8 is the variance of the density field convolved with a top-hat window of radius $8h^{-1}$ Mpc used to normalize the power spectrum). This is very close to the ‘concordance’ Λ CDM model in dynamical properties. We are interested here in the dynamical evolution of the density profile and its dependence on the merging history and therefore the results obtained here are valid also in a Λ CDM cosmology. The code was tested in the cosmological context using the Santa Barbara Cluster model (Frenk et al. 1999).

A series of linear constraints on the initial density field are used to design the numerical experiments. All the constraints are of the same form, namely the value of the initial density field at different locations, and evaluated with different smoothing kernels. We used Gaussian kernels for the smoothing procedure, where the width of the kernel is fixed so as to encompass a mass M (the mass scale on which a constraint is imposed). The set of mass scales and the location at which the constraints are imposed define the numerical experiment.

Assuming a cosmological model and power spectrum of the primordial perturbation field, a random realization of the field is constructed from which a constrained realization is generated using the Hoffman & Ribak (1991) algorithm. Many different realizations of the same experiment can be performed (Romano-Díaz *et al.* in prep.).

3. MODELS

A set of five different models, *i.e.*, experiments, is designed here to probe different merging histories of a given $10^{12}h^{-1}M_\odot$ halo in an OCDM cosmology. This halo is

then constrained to have different substructure on different mass scales and locations designed to collapse at different times. The spherical top-hat model is used here to set the numerical value of the constraints. The model provides the collapse time of substructures as a function of the initial density. This is used only as a general rough guide as the various substructures are neither spherical nor isolated. Furthermore, the few constraints used here do not fully control the experiments. The nonlinear dynamics can in principle affect the evolution in a way not fully anticipated from the initial conditions. Even more important is the role of the random component of the constrained realizations (Hoffman & Ribak 1991). Thus depending on the nature of the constraints and the power spectrum assumed, the random component can provide other significant substructures at different locations and mass scales. This can be handled by adding more constraints and varying their numerical values.

Our models are designed as follows: Model A (our benchmark model) is based on two constraints. One is that of a $10^{12}h^{-1}M_\odot$ halo at the origin designed to collapse at $z_{\text{coll}} = 2.1$. This halo is embedded in a region (2nd constraint) corresponding to a mass of $10^{13}h^{-1}M_\odot$ in which the over-density is zero — a region corresponding to an unperturbed Friedmann model. This is a scale larger by about a factor of three (in mass) than the computational sphere and therefore the constraint cannot be exactly fulfilled, yet it constrains the large scale modes of the realizations to obey it. These two constraints are imposed on all other models. Model B adds two substructures of mass $5 \times 10^{11}h^{-1}M_\odot$ within the $10^{12}h^{-1}M_\odot$ halo, designed to collapse by $z_{\text{coll}} = 3.7$. Model C further splits each one of the $5 \times 10^{11}h^{-1}M_\odot$ halos into two $2.5 \times 10^{11}h^{-1}M_\odot$ substructures ($z_{\text{coll}} = 5.7$). Thus, the benchmark halo is design to follow two major mergers events on its way to virialization. Model D takes the Model A and imposes six different small substructures of mass $10^{11}h^{-1}M_\odot$ scattered within the big halo, designed to collapse at about $z_{\text{coll}} = 7.0$. Model E attempts to simulate a more monolithic collapse in which a nested set of constraints, located at the origin, is set on a range of mass scales down to $M = 10^{10}h^{-1}M_\odot$ ($z_{\text{coll}} = 6.9$). All models have been constructed with the same seed of the random field. All the density constraints constitute $(2.5 - 3.5)\sigma$ perturbations (where σ^2 is the variance of the appropriately smoothed field), and were imposed on a cubic grid of 128 grid-cells per dimension (Romano-Díaz *et al.*, in prep.). We evolve the linear initial density field from $z = 120$ until $z = 0$ by means of the FTM code. Since we want to follow as close as possible the merging history of our models, we have sampled the system’s dynamical evolution with 165 time outputs spaced logarithmically in the expansion parameter a . Each halo is resolved at $z = 0$ with around 1.2×10^6 particles within the virial radius.

4. RESULTS

All models differ substantially at early epochs, with a subsequent convergence in some of their properties but not in others. They lead to the formation of a single object of mass $\sim 10^{12}h^{-1}M_\odot$ via mergers with the surrounding substructure and with a slow accretion. To analyze the clumpy substructure we define the DM halo(s) as having the mean density equal to some crit-

ical value Δ_c times the critical density of the universe, where Δ_c depends on the redshift and the cosmological model. The top-hat model is used to calculate $\Delta_c(z)$ and the density is calculated within a virial radius (R_{vir}). The halos are identified initially by the HOP algorithm (Eisenstein & Hut 1998) and approximated by means of a radius R_{vir} . Comparison of the HOP halos with those of the standard FoF halo finder (Davis et al. 1985) shows good agreement. Given a group catalog, a merger tree is constructed for each model using all the snapshots.

The evolution toward the final halo is studied by tracking back in time the main branch that leads to this halo. The general picture which emerges is that of a halo undergoing phases of *slow* and ordered evolution intermitted by episodes of rapid mass growth *via* collapse and *major mergers*, in agreement with previous simulations (*e.g.*, Wechsler et al. 2002; Zhao et al. 2003). These are referred to as the quiescent and violent phases.

The structure of a halo is studied by fitting it to an NFW profile (Eq. 1) and following the cosmological evolution of the NFW parameters, namely R_s, R_{vir} . Note, that within a given cosmology and per a given halo of a given mass, only R_s is a free parameter to be fitted. The fitting algorithm used here is based on logarithmic binning of the halo into spherical shells, and estimating R_s by minimal χ^2 , where the residual in a given shell is normalized by its own density. The fitting is performed within $\min(0.6R_{\text{vir}}, 0.5d_{\text{H}})$, where d_{H} is the distance to the nearest massive halo. Although the spherical symmetry of a NFW model ignores some of the dynamical properties of a halo, we use it as the first approximation to the halo structure. The NFW profile is found to be a very good fit to the spherically-symmetric density in the quasi-static phases. During the violent phases, such as mergers of two almost equal mass halos or collapse of a few substructures to form a single halo, the halos are out of equilibrium and the NFW fit is only approximate.

The cosmological evolution of R_s and R_{vir} of the main halo for all the models is presented in Fig. 1. The R_{vir} trajectories (*i.e.*, the accretion trajectories) show a regular behavior and a linear growth, separated by sudden increases, all of which are associated with the violent phases. Most strikingly, R_s remains *constant* in the quiescent phases and grows *discontinuously* in the violent ones. The R_s is subject to a $\sim 5\% - 10\%$ jitter in the quiescent phases which grows stronger during the violent phases when the halos get out of a dynamical equilibrium. The scale density ρ_s shows a similar behavior, but in the opposite sense — remaining constant in the quasi-static phases and decreasing abruptly in the violent ones. We note that all models, except B, converge to the same value of R_s (within the jitter) at the present epoch of $a \sim 0.8 - 1$, in spite of the different tracks leading to it. In Model B, the two major halos have already turned around but have yet to merge. Even before this last merger, R_s is larger than in other models and is expected to grow further.

The present simulations show that there is no clear relation between ρ_s and the formation time of the halo, as given by the time of the last violent event. This contrasts with previous claims about such a correlation. The order of models given by the formation time of their halos is B, E, A, D, and C. All the models have similar ρ_s except for Model C which has a value twice as large (Fig. 1).

The evolution of the dynamical state of the main halos has been analyzed in terms of the internal kinetic energy (K) within R_s and R_{vir} . Any perturbation in the halo’s internal state (violent mass aggregation, random energy acquisition, etc.) will be reflected in its K behavior. We find that K within R_s behaves similarly to R_s — remaining constant during the quasi-static stages (within the jitter) and growing discontinuously at the violent phases. This implies a possible direct relation between the internal kinetic energy and R_s . This has been tested by comparing the relative changes of K and R_s (Figure 2), which shows that the larger is the change in K the more R_s increases. (Further analysis of this relation is to be presented elsewhere.) The internal kinetic energy computed within R_{vir} shows a similar behavior but grows very slowly during the quasi-static phases.

5. DISCUSSION

The halo growth can be divided into the violent and quiescent phases analyzed in our superior time sampled N -body simulations using constrained realizations. This allowed us to show conclusively the details which have been hinted about in the literature so far. In this *Letter* we focus on the evolution of R_s and R_{vir} leaving more comprehensive analysis for elsewhere (Romano-Díaz *et al.*, in prep.). First, we find that the NFW scale R_s stays constant during the quiescent phase and changes abruptly during the violent one. In contrast, R_{vir} is growing linearly in the quiescent and abruptly during the violent phases. Second, ρ_s stays unchanged during the quiescent phase and drops abruptly during the violent phase. Third, the value of R_s reflects the violent merging history of the halo, and depends on the number of violent events and their fractional magnitudes, independent of the time and order of these events. The corollary is that ρ_s does not reflect the formation time of the halo. Fourth, the fractional change in R_s is a nonlinear function of the fractional absorbed kinetic energy within R_s in a violent event. We note, that the accretion trajectories in all models converge to the same value. This is a reflection of the large-scale structure shared by all the models and imposed by the constrained initial conditions.

The advantage of the constrained realizations lies in the unique ability to generate a series of models with one or more parameters varied in a controlled manner, while all others are held fixed. It allows us to cleanly separate the cause-and-effect relationship between the initial parameters and the outcome of the dynamical evolution. This complements the prevailing method of large-scale cosmological simulations in which issues of structure and evolution are addressed statistically. The scaling relations found in such a statistical analysis are not necessarily applicable to an individual halo. Here we focus on the role of the merging history in the halo evolution, by imposing density constraints based on the top-hat model. We find that the actual history of a halo does not always follow closely the expectations based on the simple top-hat model. In spite of this the different models provide us with a good laboratory for experimenting with the role of the merging history in shaping the structure of DM halos.

The analogy between the halo evolution and thermodynamical processes has not escaped our attention. Equating the quiescent phases with adiabatic processes and the

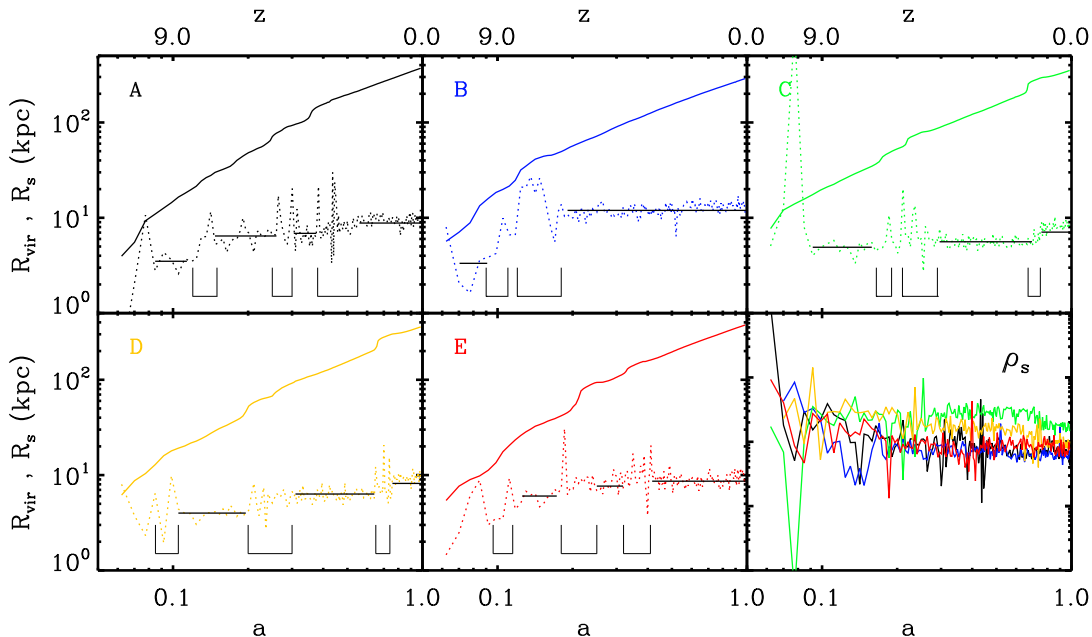


FIG. 1.— Virial and scale radii behavior (continuous and dotted lines respectively) as function of a for models A, B, C, D and E. The discontinuous growths in R_s and R_{vir} match the violent phases that each halo passes through. The horizontal bars represent the mean value of R_s within the quiescent phases. The square brackets delineate the violent phases. The bottom right panel shows the evolution of ρ_s with colors corresponding to the models in other panels.

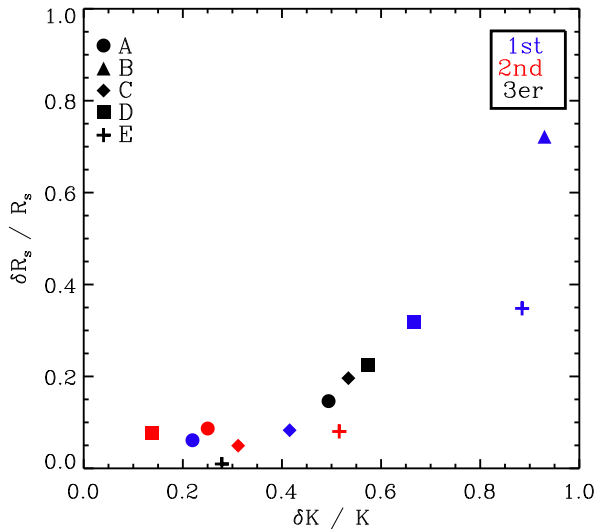


FIG. 2.— The fractional variations in the internal kinetic energy $\delta K / K$ vs those in the scaling radius $\delta R_s / R_s$ before and after the violent phases. The colors correspond to different generations of major mergers.

violent with non-adiabatic ones leads one to associate the behavior of R_s with that of the entropy. In this terminology the entropy remains constant in the quiescent phase and grows discontinuously in the violent phase (see Fig. 2). Also, the accretion trajectories play the role of adiabats and the system jumps from one adiabat to the other by a violent event, not unlike a shock wave. The question whether this is just a simple analogy or provides a deeper understanding will be addressed elsewhere.

The results obtained here pertain to the one halo studied in the framework of an Λ CDM cosmology. Yet, the conclusions reached from the set of experiments presented here are relevant to the understanding of halo formation in the general CDM cosmologies and in particular to the ‘benchmark’ Λ CDM cosmology.

This research has been partially supported by ISF-143/02 and the Sheinborn Foundation (YH), by NSF/AST 00-98351 and NASA/NAG 5-13275 (AF), by NASA/LTSA 5-13063, NASA/ATP NAG5-10823, HST/AR-10284 (IS), and by NSF/AST 02-06251 (CH & IS). ERD has been partially supported by the Golda Meier fellowship at the HU. We acknowledge fruitful discussions with A. Klypin & R.v.d. Weygaert.

REFERENCES

- Ascasibar, Y., Yepes, G., Gottlöber, S., Müller, V. 2004, MNRAS, 352, 1109
 Barnes, J., Hut, P. 1986, ApJ, 324, 446
 Bertschinger, E. 1985, ApJS, 58, 39
 Davis, M., Efstathiou, G., Frenk, C. S., & White, S. D. M. 1985, ApJ, 292, 371
 Dehnen, W. 2002, J. Comp. Phys., 179, 27
 Eisenstein D. J., Hut P., 1998, ApJ, 314, 137
 El-Zant, A. A. 2005, MNRAS, submitted, astro-ph/0502472
 Fillmore, J.A., Goldreich, P., 1984, ApJ, 281, 1
 Frenk, C.S. et al. 1999, ApJ, 525, 554
 Gunn, J. E. 1977, ApJ, 218, 592
 Heller, C.H., Shlosman, I. 1994, ApJ, 424, 84
 Heller, C.H. 1995, ApJ, 455, 252
 Hoffman, Y., Ribak, E. 1991, ApJ, 380, L5
 Hoffman, Y., Shaham, J. 1985, ApJ, 297, 16
 Lokas, E., Hoffman, Y. 2000, ApJ, 542, L139
 Moore, B., et al. 1998, ApJ, 499, L5
 Navarro, J. F., Frenk, C. S., White, S. D. M. 1996, ApJ, 462, 563

- Navarro, J.F., Frenk, C.S., White, S.D.M. 1997, ApJ, 490, 493 (NFW)
- Nusser, A. 2001, MNRAS, 325, 1397
- Nusser, A., Sheth, R. 1999, MNRAS, 303, 685, 1397
- Salvador-Solé, E., Manrique, A., Solanes, J.M. 2005, MNRAS, 358, 901
- Wechsler, R. H., *et al.* 2002, ApJ, 568, 52
- White, S. D. M. 1976, MNRAS, 177, 717
- Zel'Dovich, Y. B. 1970, A&A, 5, 84
- Zentner, A. R., Bullock, J. S. 2003, ApJ, 598, 49
- Zhao, D. H., Jing, Y. P., Mo, H. J., Börner, G. 2003, ApJ, 597, L9